Optimizing the subcritical water valorization of insect (*Hermetia illucens l.*) farming waste for biodiesel production

Oseweuba Valentine Okoro[1*], Victor Preat[1], Keikhosro Karimi[2,3], Lei Nei[4], Frederic Debaste[5], Amin Shavandi[1*]

[1]Université libre de Bruxelles (ULB), École polytechnique de Bruxelles - BioMatter unit, Avenue F.D. Roosevelt, 50 - CP 165/61, 1050 Brussels, Belgium.

[2] Department of Chemical Engineering, Vrije Universiteit Brussel, 1050, Brussels, Belgium

[3] Department of Chemical Engineering, Isfahan University of Technology, Isfahan, 84156-83111, Iran

[4]College of Life Sciences, Xinyang Normal University, Xinyang 464000, China

[5]Université libre de Bruxelles (ULB), École polytechnique de Bruxelles - Unit in Transfers, Interfaces and Processes, Avenue F.D. Roosevelt, 50 - CP 165/67, 1050 Brussels, Belgium.

Abstract

To counter the proliferation of secondary waste streams generated on insect (black soldier fly) farms, the present study integrated green water technology and acid-catalyzed transesterification as a basis to assess further value extraction potentials. By valorizing the waste streams, a process was developed to promote the circular economy paradigm. In this regard, wastes generated from a local insect farm were initially subjected to subcritical water extraction (SWE) for lipid recovery. The SWE process was optimized such that an enhanced lipid yield of 13.31 wt.% was obtained at temperature, time, and solid loading conditions of 236.8 °C, 10 min of extraction, and 1 g/ 100 mL respectively. The lipids recovered were then subjected to an acid-catalyzed transesterification reaction for the production of a fatty acid methyl ester (FAME) mixture. A preliminary economic assessment of the process was also undertaken. The results showed that the wastes had the potential to be economically employed in the production of biodiesel that satisfied fuel property standards. In addition, the potential of employing the side streams as an animal feed was also highlighted due to the determined dominance of oligopeptides, which are known for their favorable bioactive properties. The results indicated that insect farming waste is a promising renewable source for high-quality biodiesel and animal feed production through the environmentally friendly biorefinery.

Keywords: biodiesel, black soldier fly wastes, circularity, lipid, sustainable biowaste management

1 Introduction

The proliferation of insect (e.g., black soldier fly) farms has been observed largely due to their reduced potential for generating greenhouse emissions, low impact on the environment, and low requirement for resources necessary for insect growth (Baicu, 2022). These black soldier fly (BSF) farms have the capacity to process highly polluting organic waste streams (e.g., kitchen residues, manure) by facilitating high biomass reduction rates of up to 80 wt.% (Dortmans et al., 2017; Myers et al., 2008; Purkayastha & Sarkar, 2021; Surendra et al., 2020; Zhou et al., 2013). The mass reduction occurs due to the use of the organic waste streams as a nutrient source for insect larva growth, which can constitute a valuable feed for animals (Wang et al., 2017). Additionally, since BSFs do not carry disease and are incapable of biting and stinging (Bogusz et al., 2022; Lalander et al., 2019), their use for organic waste management via the bioconversion of the waste to important biomolecules (e.g., lipids) is promoted (Liu et al., 2022). Indeed, the BSF larva has been widely employed as a source of edible proteins in the so-called "BSF farms" (Nguyen et al., 2018; Su et al., 2019; Zheng et al., 2012). While the potential of utilizing the BSF as a 'bio processor' is well known, the proliferation of such farms has also increased the challenge of secondary waste management issues. This is because of the associated generation of waste residues composed of dead adult flies, puparia, and flakes from the farms (Insect farm personal communication, April 3, 2022). The valorization of these waste streams is therefore crucial to unlocking the full potential of the BSF farms via their valorization to high-value products (Caligiani et al., 2018; Ravi et al., 2020). This situation will enhance the achievement of a zero-waste bioeconomy for promotion of the circular economy (Madau et al., 2020). The circular economy is a paradigm that aims to minimize waste and promote human life sustainability by focusing on the replacement/reducing non-renewable sources, e.g., fossil-based chemicals and fuels. The circular economy paradigm is gaining traction globally as a way to address the environmental challenges of our time, such as climate change, resource depletion, and waste management (Yang et al., 2023). It is being embraced by governments, businesses,

and individuals as a way to create a more sustainable future via the valorisation of wastes to produce renewable fuels such as biodiesel, which can serve as alternatives to non-renewable fuels.

Biodiesel is a monoalkyl ester of fatty acid that can be produced from lipids via several methods such as pyrolysis, transesterification, and micro emulsification, with transesterification constituting the most common approach (Suzihaque et al., 2022). It is a carbon-neutral, low emission and biodegradable fuel that can serve as a sustainable substitute for fossil-sourced diesel (Pandey et al., 2022). The use of insect farming wastes as feedstocks for biodiesel production enables the reduction in global consumption of fossil crude which was reported to be ~ 11.7 billion tons of oil equivalent in 2018 (Jung et al., 2022). The biodiesel produced also reduces the rapid depletion of fossil reservoirs for the mitigation of existing pollution and global warming issues (Oh et al., 2018). The present work explores the subcritical water (SWE) technology for lipid recovery as an alternative to the conventional approaches that employ toxic organic solvents for extraction since SWE is recognized as green and environmentally friendly (Park et al., 2022). Indeed, water employed in SWE is regarded as safest solvent, especially since the bioproducts could be employed as an alternative animal feed. Subcritical water has the capability to dissolve polar molecules by temporarily decreasing its dielectric constant, thus making it an effective solvent for lipid extraction (Park et al., 2022). It is important to acknowledge that all existing works in the literature focus on the use of the BSF larvae farm product as a feedstock for biodiesel production. Notably, in the studies by Jung et al. (2022) and He et al. (2022), biodiesel was produced using the lipids sourced from BSF larvae via the KOH-catalyzed and the enzyme-catalyzed transesterification processes, respectively, with yields of > 90 wt.% determined in both cases. Crucially, in all existing studies of biodiesel production from BSF, the consideration of its associated secondary waste streams as potential feedstocks for biodiesel production are yet to be explored in the literature. To this regard, SWE for lipid recovery from the insect farming waste streams was optimized prior to biodiesel

production. The optimization of process conditions for enhanced lipids recovery from the waste samples was undertaken using the Box-Behnken design (BBD) method.

This work predicted the biodiesel properties of the insect farming waste biodiesel based on the fatty acid alkyl ester composition. This is because, the properties of biodiesel are a function of the composition of its component neat fatty acid alkyl esters, with the use of the classic mixing rule typically employed as a *priori* estimation approach (Benjumea et al., 2008). Finally, a preliminary economic assessment of the biodiesel production process was undertaken as a basis for assessing overall functionality. The novelty of this study is therefore highlighted by the attempt to bridge the existing knowledge gap with respect to insect farming waste valorization for biodiesel production, while simultaneously assessing the biodiesel properties and the preliminary economic viability of the process. To the best of our knowledge such a study is yet to be undertaken in the literature.

2 Materials and methods

2.1 Sample collection and storage

The waste samples (i.e., adult insects, puparia, and flakes) were provided by an insect farm that rears BSF using mainly fruit and vegetables as the substrates for larva production. The acquired samples were stored in zipped plastic containers at -20°C in a freezer prior to undertaking experimental investigations.

2.2 Characterization of dead adult flies, puparia and flakes samples

The waste samples were initially dried to constant mass and then finely ground to $x < 0.5$ mm prior to undertaking proximate and ultimate analyses. The proximate analysis of the waste samples was undertaken to determine fixed carbon, moisture, ash, and volatile matter contents using ASTM standard methods (ASTM, 1998; ASTM, 2007; ASTM, 2015; ASTM, 2011). Ultimate analysis for the determination of carbon (C), hydrogen (H), nitrogen (N), and sulfur (S) contents of the samples were also undertaken using an elemental analyzer (LECO TruSpec

CHN, Saint Joseph, Michigan, USA). Additional analyses for the determination of lipid and protein contents of the samples were undertaken using the Soxhlet method (Hobbi et al., 2023; Kim et al., 2012) and AOCS official method Ba4e-93 (AOAC, 1998), respectively. The total carbohydrate content was measured using AOAC official method (AOAC, 2012). Our previous work, focusing on chitin content of these waste streams had determined that the puparia, flakes and adult insect fractions present mean chitin contents of 27 wt.%, 24 wt.%, and 10 wt.%, respectively (Brigode et al., 2020).

2.3 Subcritical water extraction of lipids

To enhance the recovery of lipids from the waste samples, SWE was employed and the influence of the important process parameters of temperature, extraction time, and solid loading, was investigated (Haghighi & Khajenoori, 2013; Reddy et al., 2014). The dried and finely ground samples were initially mixed in equal proportions by mass. The selected process parameters were then investigated for ranges of 150-250 °C for the temperature, 10 -30 min of extraction time, and 1-15 w/v% solid loading. These ranges were selected based on optimal ranges of the parameters reported in previous works that employed SWE in the recovery of lipids from biomass (Akhtar & Amin, 2011; Ho et al., 2018; Pavlić et al., 2016; Polikovsky et al., 2020; Reddy et al., 2014; Rodríguez-Meizoso et al., 2010; Zeković et al., 2014).

2.3.1 Design of experiments

Based on the ranges of the process parameters selected, their values were encoded with levels ranging from -1 to +1, as presented in Table 1.

Table 1: Process parameters and associated coded levels

Levels	Temperature (°C)	Solid loading (g/100mL)	Time (min)
-1	150	1	10
0	200	8	20
+1	250	15	30

To undertake the SWE, the finely ground waste mixture containing adult insect, puparia, and flakes in the mass ratio of 1:1:1 was introduced to a 50 mL high-pressure stainless-steel reactor (Xiamen Ollital Technology Co., Ltd., China) and the appropriate volume of water added to achieve a solid loading in accordance with the BBD model, and the reactor sealed. The reactor was then purged for ~60 s using nitrogen to remove air in the reactor headspace after which it was heated to the target temperature, for a specified time of extraction in accordance with the BBD levels. After completing the experiments, the reactor was cooled using cold water. The extracted lipid was then recovered from the aqueous phase using hexane (1:1 v/v ratio) and the extract was transferred to centrifugation tubes. The tubes were then vigorously stirred using a vortex mixer with the top hexane layer, containing the dissolved lipids subsequently recovered and dried to constant mass at 60 °C. The yield of the lipid recovered was then calculated as follows;

$$Y_l = \frac{m_l \times 100}{m_s} \tag{1}$$

where m_l denotes the mass in g of the lipid recovered and m_s represents the mass of the insect farming waste sample.

Based on the BBD, the number of experimental runs (N) was determined as follows (Velayi & Norouzbeigi, 2023);

$$N = 2k(k-1) + C_0 \tag{2}$$

where N is the number of replicates, k is the factorial number (i.e., the number of variables) and C_o is the replicate of the central points.

2.3.2 Empirical model development

The generated data subsequently analyzed using Minitab® 17.1.0 (Minitab, Inc. USA) and a second-order polynomial model developed and presented as follows;

$$Y_l = X_0 + \sum_{i=1}^{3} b_i X_i + \sum_{i=1}^{3} b_{ii} X_i^{\,2} + \sum_{i=1}^{3} \sum_{j=1} b_{ij} X_i X_j \quad (3)$$

where Y_l represents the yield of the lipid extracted in wt. %, X_o represents the model intercept, X_i (X_j) represents the ith (jth) process parameters (temperature, time, solid loading), b_i, $b_{ii,}$ and b_{ij} represent the model regression coefficients.

The second-order polynomial model that best describes the SWE process was then employed in assessing the impacts of the process parameters and the associated significance of the impacts using ANOVA. The Minitab® Software was then employed in estimating the conditions of the process variables for optimum lipid yield using the in-built desirability function (Costa et al., 2011; Derringer & Suich, 1980) and the accuracy of the predicted conditions for optimum lipid yield subsequently assessed using the relative absolute deviation (RAD) metric defined as follows (Okoro et al., 2017a);

$$RAD = \left| \frac{Y_{l,\exp} - Y_{l,pre}}{Y_{l,\exp}} \right| \quad (4)$$

where $Y_{l,exp}$ represents the experimental yield of the lipid, $Y_{l,\,pre}$ denotes the predicted yield of the lipid.

2.3.3 Aqueous phase analysis

Due to the potential of employing the aqueous phase (i.e. after lipid extraction), as a source of bioactive proteins for animal feed, SDS-page was undertaken to determine the presence of proteins and the protein molecule size (Brunelle & Green, 2014). The aqueous phase sample was therefore initially freeze-dried in the I-5 model furnished by Christ ® at -35°C for two days after which 0.015g of the dried sample was dissolved in 1 mL of milli-Q water, with the dissolution enhanced using a drop of 20 wt.% NaOH. The mixture was then heated for 5 min

in a marine bath. After heating the mixture was cooled and analyzed via electrophoresis, using a NovexTM gel for 1 h at 150V. The protein standard used was the Seeblue plus2 pre-stained with a ladder from 3-198 kDa (Brunelle & Green, 2014). In this study all experimental runs were undertaken in duplicate with mean values reported.

2.4 Fatty acid methyl esters (FAMEs) production using extracted lipids

The transesterification of the extracted lipids was undertaken via an acid catalyzed process in an attempt to counter the risk of unwanted saponification reactions in the presence of fatty acids (FAs) (i.e. >1 wt.%) when the conventional base catalyst is employed (Okoro et al., 2017b). This is because there is an enhanced risk of FA formation via lipid hydrolysis during the moderate-high temperature SWE process. To this regard, the protocol for acid-catalyzed transesterification, reported in the literature was employed (Ehimen et al., 2010). Briefly, 2 g of optimally extracted lipid was reacted with 30 mL of methanol containing 0.02 mol of H_2SO_4. The reaction was then undertaken for 8 h at 60 °C and with constant stirring at 500 rpm, using a magnetic mixer in a batch reactor vessel. The resulting fatty acid methyl ester (FAME) mixture from the insect farming or BSF waste stream has been designated as BWME henceforth for simplicity. This BWME was subsequently recovered utilizing hexane. The BWME profile was determined via gas chromatography. The GC equipment was equipped with a 7683 autosampler coupled with a flame ionization detector (FID). 1 µL of the BWME dissolved in hexane, was injected into the HP-5 column in split mode at 20:1. Hydrogen was used as the carrier gas at a flow rate of 2.2 mL/min. Injector and detector temperatures were specified as 240 °C and 250 °C, respectively. The oven temperature started at 120°C and increased to 225 °C with 3°C/min rate. Once 225 °C was reached, the temperature was programmed to increase at a rate of 10 °C/min till the maximum temperature of 245°C was attained. Experimental data were then analyzed using the Chemstation software with the peaks identified using standard peaks. The qualitative molar fraction of each FAME was then estimated via “area” analysis of the chromatographic output.

2.5 Biodiesel properties estimation

Since chain length, branching, and unsaturation of the FAMEs constitute structural features that can influence the fuel properties of the biodiesel (Knothe, 2005; Okoro et al., 2017a), the FAME profile or composition can be employed in predicting crucial biodiesel properties thus saving cost and time. This was demonstrated in a previous study that utilized simple correlations, based on the composition of the FAMEs or neat esters, to predict the properties of cetane number, density and higher heating values with percentage errors of < 2% when compared to experimentally determined values of these properties (Giakoumis & Sarakatsanis, 2018). Similarly, the biodiesel properties of kinematic viscosity, density, and higher heating value (HHV) were shown to be predictable based on the composition of the neat esters, with low errors of 2.57 %, 0.11 % and 0.21 % respectively when compared to the experimentally determined values (Ramírez-Verduzco et al., 2012). The cold flow properties of biodiesel were also reported to be accurately predicted using the neat fatty acid alkyl ester composition with correlation coefficients of >96 % reported in studies undertaken in the literature (Ramos et al., 2009; Sarin et al., 2009). Okoro et al. (2017a) also illustrated the reliability of this estimation method, showing an average absolute percentage deviation lower than 5%, between the predicted and the measured value of animal-sourced biodiesel. In this regard, the properties of density, viscosity, cetane number (CN), cloud point (CP), cold filter plugging point (CFPP), flash point (FP), and HHV (Hoekman et al., 2012) were selected and estimated due to their impact on fuel performance.

Notably, the higher CN, the shorter time needed for the component to auto-ignite (Knothe, 2005). Other properties of HHV, kinematic viscosity, and density constitute crucial properties of a fuel since they dictate its energy content or density and the degree of fuel atomization, respectively (Knothe, 2005). It must be noted that the low-temperature flow behavior of fuel constitutes a crucial consideration in assessing the suitability of a fuel in diesel engines since a poor low-temperature performance may lead to wax crystal formation and subsequent engine

starving or filter plugging. This low-temperature flow behavior is typically measured using the CFPP and the CP properties (Hoekman et al., 2012; Knothe, 2005).

In the present study, density, viscosity, CN, CP, CFPP, FP, and HHV of the BWME mixture were estimated using kay's mixing rules as follows Okoro et al. (2017a);

$$\phi = \sum_{i}^{n} X_i \phi_i \tag{5}$$

where ϕ represents the estimated property ϕ_i the respective property of the *i*th component (FAME), and X_i represents the molar fractions of the *i*th FAME.

Similarly, to determine the CP and CFPP of the BWME mixture recent studies have proposed several empirical models based on the FAMEs fractions (Agarwal et al., 2010; Alviso et al., 2020; Clements, 1996; Sarin et al., 2009). The present study, therefore, employed the empirical relation as follows (Clements, 1996);

$$\ln(CP + 10) = 2.2 - 1.57 \sum_{i}^{n} U_i \tag{6}$$

where U_i represents the mole fraction of the *i*th unsaturated FAME and *CP* is the cloud point temperature in °C.

The CFPP temperature was subsequently estimated from the CP temperature as follows (Dunn & Bagby, 1995);

$$CFPP = 1.0191 \times CP - 8.1172 \tag{7}$$

where *CFPP* is the cold filter plugging point temperature in K and *CP* is the cold point temperature in K.

Finally, The flash point of the FAME mixture was calculated based on the estimated kinematic viscosity as follows (Demirbas, 2007);

$$FP = 32.641v + 302.02 \quad (8)$$

where FP is the flashpoint in K and v denotes the kinematic viscosity of the FAME mixture in mm^2/s

2.6 Preliminary economic assessment of the biodiesel production process

To assess the economic performance of the proposed process for biodiesel production, the unit processing cost of the insect farming waste (U_{IFW} in US$/kg) for a moderate waste processing capacity of 100 kg/h was calculated. The calculations were based on the simplified flow diagram presented in Figure 1.

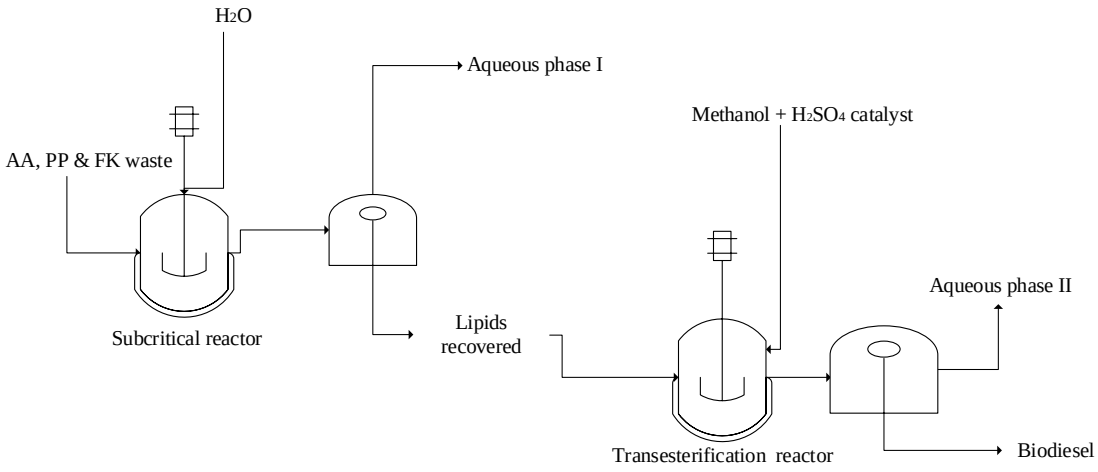

Figure 1: Simplified flow diagram of the proposed biodiesel production process. AF, PP, and FK denote dead adult flies, puparia, and flakes, respectively. Aqueous phases I and II contain dissolved molecules such as proteins and glycerol that can be employed as animal feed and a valuable biochemical, respectively.

The U_{IFW} was then compared to the unit cost of disposing organic waste in landfills (mean value of US$ 0.133/kg in Belgium) since most waste management approaches are based on the use of landfills (EEA, 2013; worldbank, 2023). The unit processing cost of the insect farming waste was calculated using approximate methods adapted from the literature as follows (Okoro et al., 2019);

$$U_{IFW} = \frac{C_{AC} + C_{AOP} - R_b}{m_T} \tag{9}$$

where C_{AC} is the annualized capital cost in $US determined as follows;

$$C_{AC} = I_{2022} \times \left[\frac{(1+i)^n \times i}{(1+i)^n - 1} \right] \tag{10}$$

and

$$I_{2022} = 1.81 \times E_{ISBL,2022} \tag{11}$$

and

$$E_{ISBL,2022} = f_L \sum_{i}^{n} C_{eq-i} \tag{12}$$

where $C_{eq\text{-}i}$ is the purchase cost of the *i*th equipment in US$.

The costs of the equipment namely SWE reactor (C_{SWE}), FAME production reactor (C_{FAME}) and the separation tanks (C_T) in US$ were estimated as follows;

$$C_{SWE} = 1.5\left(13,000 + 34,000 v_R^{\,0.5}\right) \tag{13}$$

$$C_{FAME} = 14000 + 15400 v_R^{0.7} \tag{14}$$

$$C_T = 5700 + 700 v_T^{0.7} \tag{15}$$

To account for the inflation effects on money, the purchase costs were adjusted using CEPCI factors of 776.9 and 499.6 for years 2023 and 2006 respectively (Okoro et al., 2022).

and where C_{AOP} is the annual operating cost in $US and determined as follows (Okoro et al., 2019);

$$C_{AOC} = L_c + C_c + D_c + R_m + E_c + V_c \tag{16}$$

and

$$V_c = 0.05\left(D_c + L_c + E_c\right) \tag{17}$$

In equations above, R_b denotes the revenue from the sale of biodiesel in US$, n and i denote the project lifespan and discount rate, specified to be 30 y and 10% respectively; I_{2022} represents the capital cost in US$ for year 2022; $E_{ISBL,2022}$ is the inside battery limit equipment cost in US$ for year 2022; v_R and v_T denote the volumes of the reactor in m^3 (corrected with factor of 1.2 for overhead space) and separating tank (assumed to be 20 m^3) respectively (Okoro et al., 2022). The symbol, L_c denotes the labour cost for three workers assumed to be US$33150 per worker per year (Talent, 2023), C_c denotes the cost of chemicals consumed in US$ (methanol=US$ 0.528 per kg, H_2SO_4 =US$ 0.098 per kg (Chemanalyst, 2023; Methanex, 2023)), D_c denotes the depreciation cost determined using the straight line approach with assumed salvage value of zero; R_m denotes the repair and maintenance cost estimated as 6% of

I_{2022}; E_c is the energy (heating) cost and was specified as US$ 2.48 $\times 10^6$ per kJ and V_c denotes the overhead cost in US$; f_L denotes the lang factor specified as 3 in accordance with other similar biofuel and biodiesel studies (Humbird et al., 2011; Viswanathan et al., 2021).

The heating energy consumed per unit mass of mixture in the subcritical water extraction process was estimated as follows (Vardon et al., 2012);

$$E = \left(w_i C_{pw} T + \left(1 - w_i\right) C_{pb} T\right)\left(1 - R_h\right) \tag{18}$$

where W_i , T, C_{pw}, C_{pb} and R_h denote the fractional water content at the beginning of the experiment, the temperature increase to attain the target temperature from 25 °C, specific heat capacities of water and biomass specified as 4.18 kJ/(kg.K) and 1.25 kJ/(kg.K), respectively and the efficiency of heat recovery specified as 0.5.

For the FAME production process, the energy consumed per unit mass of mixture was estimated using similar approaches to equation (17) as follows;

$$E = \left(m_i C_{pm} T + \left(1 - m_i\right) C_{po} T\right)\left(1 - R_h\right) \tag{19}$$

where m_i and C_{pm} denote the fractional methanol content at the beginning of the experiment, the temperature increase to attain the target temperature from 25 °C, specific heat capacity of methanol was specified as 2.53 kJ/(kg.K)(EngineeringToolBox, 2018). The symbol of C_{po} denotes the specific heat capacity of the fatty acid mixture, with the specific heat of the dominant fatty acid (from FAME analysis) employed as the representative specific heat capacity of the mixture.

3 Results and discussion

3.1 Properties of the samples

The samples of puparia, flakes and adult insect employed are presented in Figure 2.

(a) (b) (c)

Figure 2 : A pictorial illustration of the (a) puparia, (b) flakes, and (c) adult insect samples

The proximate and ultimate analyses of the puparia, flakes and adult insects waste samples are presented in Table 2.

Table 2: Proximate and ultimate analyses of insect farming waste fractions

Analysis	Adult insects	Flakes	Puparia
Proximate			
Moisture (% w/w, wet basis)	7.29	7.59	10.19
Volatile (% w/w, dry basis)	85.57	87.92	83.18
Ashes (% w/w, dry basis)	3.77	2.29	5.40
Fixed carbon (% w/w, dry basis)	10.66	9.80	11.42
Ultimate analysis			
Carbon (% w/w, dry, ash-free basis)	42.18	41.57	40.28
Hydrogen (% w/w, dry, ash-free basis)	6.29	5.86	5.75
Nitrogen (% w/w, dry, ash-free basis)	5.73	6.93	5.56
Sulphur (% w/w, dry, ash-free basis)	1.67	1.11	4.96
Oxygen (% w/w, dry, ash-free basis)	44.02	44.51	43.44
Macromolecular composition			
Lipid (% w/w, dry basis)	6.92	10.41	23.75
Proteins (% w/w, dry basis)	32.83	39.57	31.74

[a]Total Carbohydrates (% w/w, dry basis)	56.48	47.76	39.11

[a]Total carbohydrates also include the chitin content

Table 2 shows that the moisture content of the samples ranged from 7.29- 10.19 wt.%. This value was lower than the moisture content of the whole BSF prepupae which typically ranges from 50 to 60 wt.% (Caligiani et al., 2018; Ewald et al., 2020). This lower moisture content in the waste streams may be due to the loss of water during heating and pressing for the flakes fractions and the drying up of the prepupae during pupations (Dortmans et al., 2017). Table 2 also shows that volatile contents of the waste fractions were comparable and ranged from 83.18-87.92 wt. %. These high volatile contents may be indicative of the poor combustion property of the waste streams if employed as a solid fuel since higher volatile contents may translate into increased carbon dioxide emission, low thermal output, and increased emission of particulate matter (Ilham, 2022). The ash contents of the waste fractions were determined to be comparable to the ash contents of the whole BSF, which typically ranges from 3-5 wt.% (Surendra et al., 2020). Table 2 shows that the three fractions have varied mean lipid contents ranging between 6.92-23.75 wt. %, highlighting the potential of using the combined insect farming waste stream as a sustainable lipid source. Additionally, the mean high protein and carbohydrate contents of 34.71 and 47.78 respectively also suggest the potential of exploring the defatted sample as a cheap animal feed or as a source of high-value biopolymer of chitin. This possibility will be explored in future studies.

3.2 Lipid recovery from the waste streams

At the end of the SWE, the lipid product was recovered using methods described earlier above, and the yields are presented in Table 3.

Table 3: Lipid yields for different experimental conditions

Exp	T (°C)	t (min)	S_l (g/100mL)	Experiment Y_l (wt. %)	Fitted Y_l (wt. %)	Residual
1	200	10	1	12	12.40	-0.4
2	200	20	8	7.63	7.70	-0.07
3	250	20	15	6.04	6.84	-0.8
4	200	30	15	8.18	7.78	0.4
5	200	20	8	7.83	7.70	0.13
6	150	10	8	4.13	4.52	-0.39
7	200	20	8	7.63	7.70	-0.07
8	250	30	8	5.05	4.66	0.39
9	150	30	8	7.73	6.93	0.80
10	150	20	1	9.2	8.40	0.80
11	150	20	15	3.44	4.64	-1.20
12	200	30	1	8	9.95	-1.59
13	200	10	15	9.48	7.89	1.59
14	250	20	1	10.6	9.40	1.20
15	250	10	8	9.2	10.00	-0.80

T, t ,S_l, and Y_l denote temperature, time, solid loading, and lipid yield respectively

Table 3 shows that the lipid yield varies from 3.45- 12 wt.%, with the data employed in the development of the second-order polynomial model presented as follows;

$$Y_l = -27.4 + 0.348T + 0.440t - 1.000S_l - 0.000653T^2 + 0.00463t^2 + 0.0256S_l^2 - 0.00387T \times t + 0.00086T \times S_l + 0.0096t \times S_l \quad (20)$$

where T, t ,S_l, and Y_l denote temperature, time, solid loading, and lipid yield respectively.

The coefficient of determination R^2 for the model was 0.852, which is higher than 0.7, reported constituting an acceptable R^2 value (Okoro et al., 2022). The second-order polynomial model was then used to develop contours planar and plots to show the dependence of the lipid extraction on the selected process parameters and presented in Figure 3 and Figure 4 respectively, in the subsequent section.

Having recovered the lipids, proteins present in the recovered aqueous phase were assessed. The SDS-page was able to show that proteins with low molecular masses of 6 kDa were present. This observation was due to the subcritical treatment leading to protein hydrolysis leading to the formation of oligopeptides. The dominance of oligopeptides, therefore, enhances the potential use as an animal feed, since high oligopeptides content is often linked to enhanced bioactive properties (Batish et al., 2020; Sánchez & Vázquez, 2017).

3.3 Main effects of the process parameters

3.3.1 Effect of Temperature

Figure 3 shows that an increase (6.13 wt.% to 8.68 wt.%) in the target temperature from 150 ^{o}C to 200 ^{o}C results in an increase in the lipid yield before a decrease (8.68 wt.% to 7.72 wt.%) from 200 ^{o}C to 250 ^{o}C. The initial increase is due to the variations in the polarity, diffusion rate, and viscosity of subcritical water as the temperature increases (Haghighi & Khajenoori, 2013). Indeed under subcritical conditions, the polarity of water reduces, enhancing the possibility of extracting lipids that may contain a non-polar hydrocarbon tail and a polar carboxylic acid head. At temperatures greater than 200 ^{o}C the decrease in the lipid yield may be attributed to the thermally induced splitting of lipids when high temperatures are imposed (Schaich, 2008).

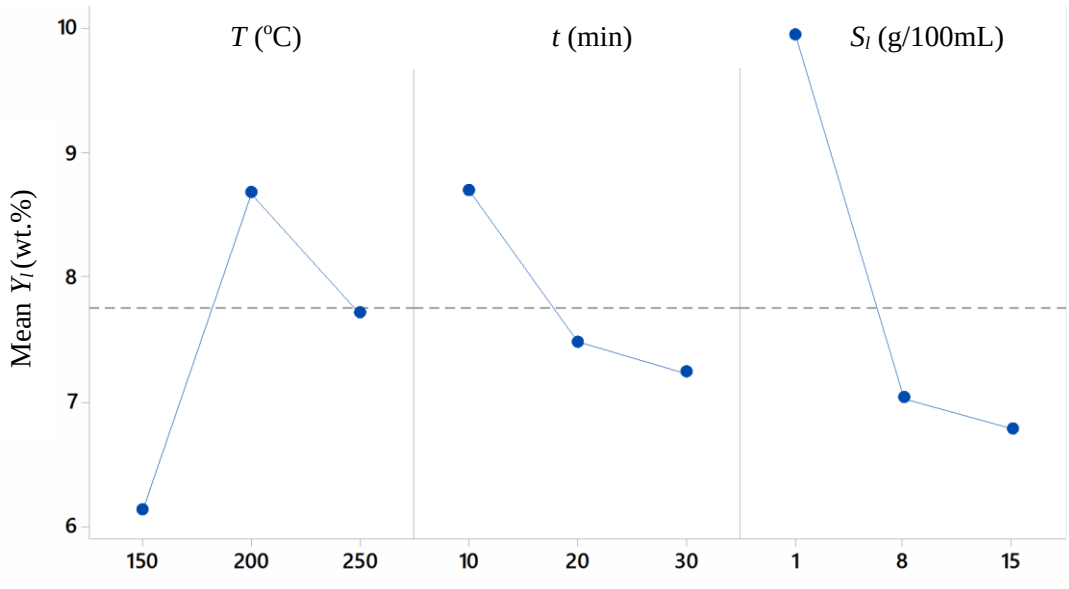

Figure 3 : The main effect plots show the statistically independent effects of the process variables of *T*, temperature (ºC), *t*, time (min) and solid to solvent ratio (g/100 mL) on lipid yield, Y_l in wt.%

3.3.2 Effect of solid loading

Figure 3 also shows that an inverse relationship exists between higher solid loading (increasing from 1 g/ 100 mL) and lipid yields (decreasing from 9.95 wt. % to 6.79 wt. %). This observation is expected due to the role of water during the process. This is because water serves as the extracting medium, implying that an increased concentration of the solids hinders the interactions between the waste mixture and the water molecules, which are crucial for mass transfer. Figure 3, therefore, shows that the preferred solid load is the lowest value investigated in the present study (i.e. 1 g/ 100 mL).

3.3.3 Extraction time

The present study also highlights a negative correlation between increasing extraction times and the yield of lipids extracted. This observation reinforces the negative effects of sustained heating on the thermal stability of the lipids extracted. Indeed it was reported that the sustained heating that occurs during long extraction times increases the risk of degradation of the lipid

molecules to short-chain, non-lipid products such as free radicals which can lead to dimer and epoxide formation (Bordin et al., 2013).

3.4 Interaction between process parameters

The contours plot shows the interaction between parameters and their impact on the lipid yield. When considering the effect of the interaction between temperature and extraction time on lipid yield when solid loading is fixed at 8 g/100mL (Figure 4a), it is observed that increasing extraction time (> 15 min) at high temperatures (> 175 ^{o}C) leads to a decrease in the lipid yield. Conversely, at temperatures near ~150 °C, extraction yield increases with increasing extraction time. The negative effects of higher temperature and time on lipid yield is because of this condition may lead to unwanted secondary reactions, implying that shorter extraction times may be preferable to optimize lipid yield when higher temperatures are imposed (Ho et al., 2018).

Similarly, if the extraction time is fixed at 20 min, the combined effect of increasing target temperature and increasing solid loading (Figure 4b), leads to an increase in lipid yield. This observation implies that the negative effect of higher solid loading on lipid yield is countered by the initial positive effect of increasing the temperature (up to 200 ^{o}C). At higher temperatures, however, the negative effects of solid loading and high temperatures (> 225 ^{o}C) on lipid yield are dominant. Figure 4c, also shows that the negative effect of higher solid loading on lipid yield is dominant irrespective of the increase in extraction time when the temperature is maintained at 200 ^{o}C. This observation reinforces the dominant influence of solid loading on lipid yield in the present study. Having investigated the impact of each parameter, the statistical significance of their independent and their combined effect were determined using experimental data presented in Table 4.

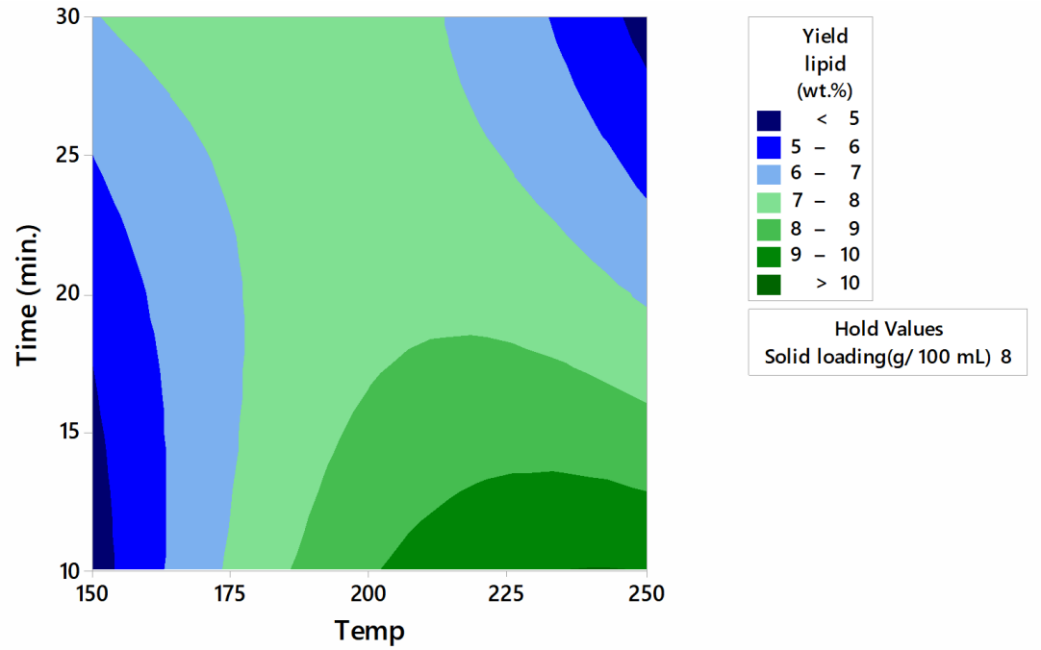

(a) Contour plot of lipid yield (wt.%) vs time (min.), temperature (°C)

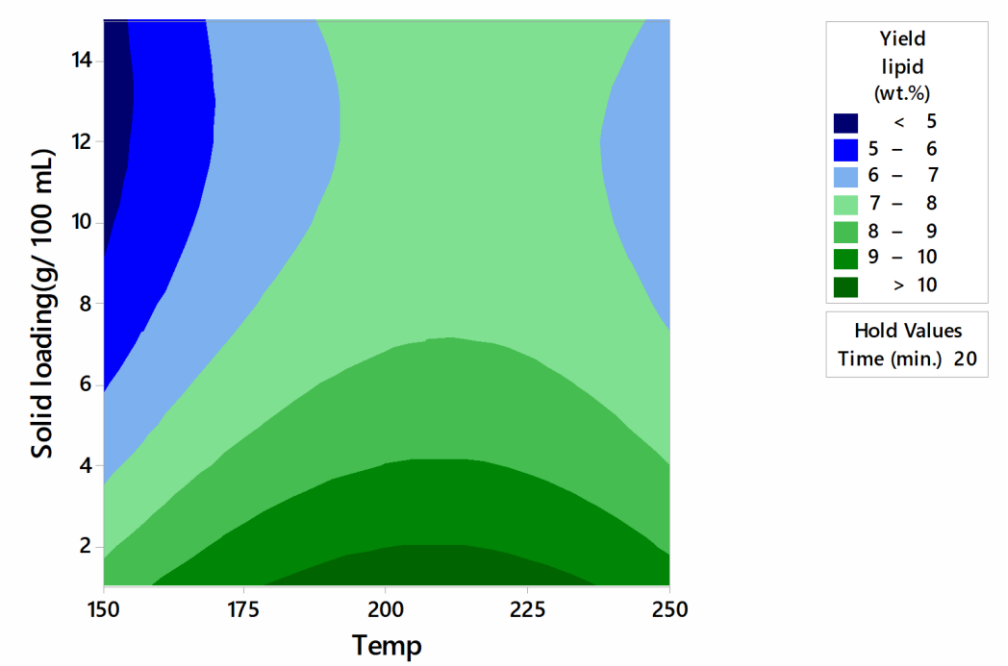

(b) Contour plot of yield lipid (wt.%) vs solid loading (g/100 mL), temperature (°C)

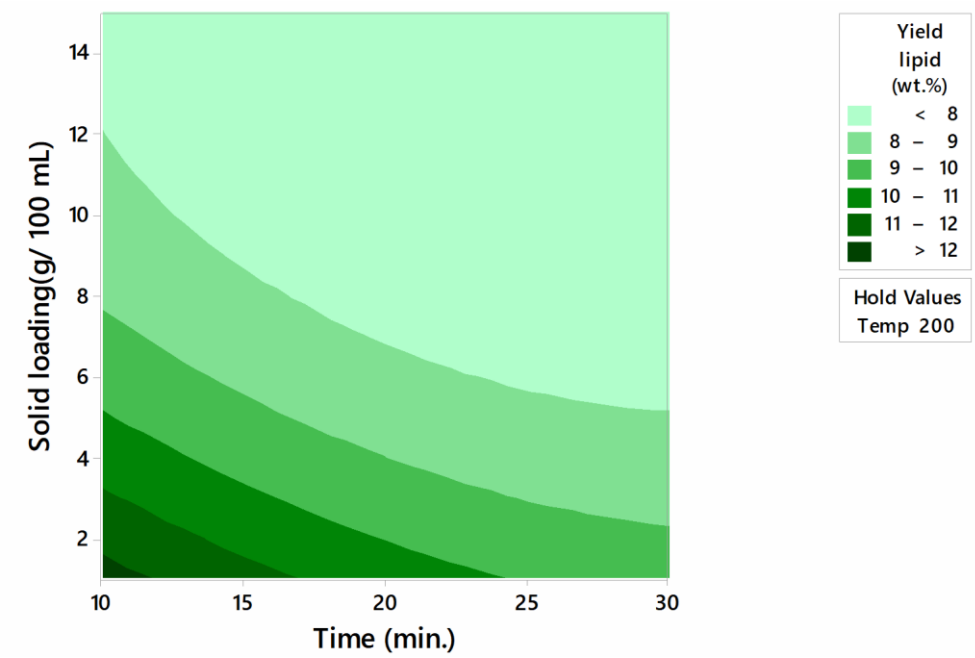

(c) Contour plot of yield lipid (wt.%) vs solid loading (g/100 mL), time (min)

Figure 4 : The combined effect contour plots of the process variables of *T*, temperature (ºC), *t*, time (min), and solid to solvent ratio (g/100 mL) on lipid yield.

3.5 Significance of effects of process parameters and optimization

In general, a p-value of < 0.05 is indicative of the high statistical significance of the process parameter on the lipid yield. Based on the p-values in Table 4, it can be concluded that solid loading is the most impacting parameter with a p-value of 0.03. Also, the impact of temperature (p-value of 0.190) was determined to be more significant than the impact of extraction time (p-value of 0.224). These observations are supported by earlier discussions presented in section 3.3. Similarly, the combined effects of temperature and time on lipid yield were shown to be significant with a p-value of 0.048.

Table 4: Statistical significance of parameters effect on lipid yield using Analysis of Variance

Parameters	DF	Adj SS	Adj MS	F-value	p-value	Significance
T	1	5.1040	5.1040	2.29	0.190	*

t	1	4.2778	4.2778	1.92	0.224	*
S_l	1	20.0345	20.0345	9.00	0.030	**
$T \times t$	1	15.0156	15.0156	6.74	0.048	**
$T \times S_l$	1	0.3600	0.3600	0.16	0.704	*
$t \times S_l$	1	1.8225	1.8225	0.82	0.407	*
T^2	1	9.8352	9.8352	4.42	0.090	*
t^2	1	0.7912	0.7912	0.36	0.577	*
S_l^2	1	5.8193	5.8193	2.61	0.167	*
Total	14					

R^2 = 0.8527; * denotes low significance; ** denotes high significance; T , t, and S_l denote temperature, time, and solid loading, respectively

Employing Minitab, the imposition of the conditions of 236.8 °C, 10 min of extraction, and 1 g/ 100 mL solid loading was predicted to achieve an optimal yield of 13.31%. This prediction has been tested experimentally and confirmed to facilitate a lipid yield of 13.2% with an associated RAD of 0.008, which is less than 0.05. This result further reinforces the suitability of the model developed.

The identified optimal temperature lies inside the investigated domain, confirming the pertinence of the investigated temperature range. For the solid loading, the optimal value is the minimal one, triggering for tests in more diluted conditions. Yet, such diluted conditions would inevitably have an impact on productivity, limiting the interest of the investigation of highly diluted conditions. For time, the optimal condition is the minimal tested condition again. As a shorter time would induce a better productivity and considering the significant coupling of time with the temperature, a further optimization of the process could be undergone by a kinetic study for times shorter than 10 minutes.

3.6 Properties of the fatty acid methyl esters (FAMEs) produced

Having undertaken the GC qualitative assessment, the FAME composition of the transesterification product is presented in Table 5. Table 5 shows that methyl laurate is the dominant FAME with a mole fraction of 0.469, followed by methyl cis-11-eicosenoate and behenate, both with a mole fraction of 0.120. The dominance of the methyl laurate is consistent with the literature since Lauric acid constitutes up to 0.60 mole fraction of the lipid present in BSF prepupae (Giannetto et al., 2020). The presence of methyl cis-11-eicosenoate and methyl behenate in the FAME mixture highlights the difference between the lipid produced in the present study compared to the lipids produced from the typical BSF prepupae since these are largely absent in BSF prepupae (Ewald et al., 2020; Giannetto et al., 2020).

The dominance of medium-chain FAMEs (Salsinha et al., 2023) is highlighted by the presence of methyl caprate (C10:0) and methyl laurate (C12:0), with a combined molar content of ~ 57%. The dominance of these medium-chain FAMEs typically translates to the lower the melting point and reduced viscosities, which may lead to favourable cold flow properties (Hoekman et al., 2012). The content of the saturated long-chain FAMEs (C16:0-C18:0) of ~7 % on a molar basis of methyl palmitate, will contribute to favourable ignition quality since ignition quality increases with enhanced saturation, branching and chain length (Cholewski et al., 2018; Islam et al., 2013; Serrano et al., 2022). Favourable ignition quality due to the presence of saturated long-chain FAMEs such as methyl palmitate may however have negative effects on the flow properties of the biodiesel product (Islam et al., 2013). It is however anticipated that the favourable effects of the medium-chain FAMES on the cold flow properties will serve to boost the overall cold flow characteristics due to the high content in the FAME profile. These cold flow characteristics will also be enhanced by the presence of unsaturated long-chain FAMEs of C18:1, C20:1, C22:1 and C24:1 since such unsaturated long-chain FAMEs can also enhance cold-flow behaviour due to their lower melting points (Islam et al., 2013). Generally speaking, the literature also reports that the HHV of the FAME presents a

positive correlation with the number of carbon atoms present in the molecule (Faizollahzadeh Ardabili et al., 2019), such that, as presented in Table 5, long-chain FAMEs have HHVs of ~39 MJ/kg $\leq x \leq$ ~41 MJ/kg while the medium-chain FAMEs have HHVs of ~35 MJ/kg $\leq x \leq$ ~37 MJ/kg. Based on the discussions presented thus far, it is observed that a converse relationship exists between the properties of the long-chain FAMEs and the medium-chain FAMEs. While the saturated long-chain FAMEs favour improved cetane numbers, their higher concentrations will lead to poor cold flow properties, with unsaturated medium-chain FAMEs presenting a converse behaviour. This implies that the preferred situation will require a balance between carbon length and saturation degree, with an optimisation study focusing on these FAMEs properties constituting an interesting future research area.

Table 5: Molar fractions of the fatty acid methyl esters from the insect farming waste and fuel properties

Compound ID	Common name	Mole fraction	HHV (kJ/kg)	Density (kg/m^3 at 15 °C)	Kinematic viscosity (mm^2/s at 40 °C)	Cetane number
C10:0	Methyl caprate	0.011	34.81[b]	872.26 [b]	1.71[b]	49.4[b]
C12:0	Methyl laurate	0.469	36.58[b]	869.46 [b]	2.39[b]	61.1[b]
C16:0	Methyl palmitate	0.069	39.45[a]	864.19 [a]	4.38[a]	85.9[a]
C16:1	Methyl palmitoleate	0.021	39.29[a]	882.39 [a]	3.67[a]	51[a]
C18:1	Methyl cis-vaccenate (cis 11)	0.018	39.91[a]	877.46 [a]	4.51[a]	59.3[a]
C18:1	Methyl oleate (cis 9)	0.095	39.91[a]	877.46 [a]	4.51[a]	59.3[a]
C20:0	Methyl arachidate	0.027	40.62[a]	866.28 [a]	7.20[b]	100[b]
C20:1	Methyl eicosenoate (cis11)	0.120	40.61[b]	873.8 [b]	5.84[b]	64.8[b]
C22: 0	Methyl behenate	0.120	41.20[c]	866.55[d]	6.88[d]	125[e]
C22: 1	Methyl erucate	0.024	40.99 [b]	870.5 [b]	7.16 [b]	76[b]
C24: 0	Methyl lignocerate	0.016	>41.2 [f]	864.82d	8.23[d]	>125[f]
C24:1	Methyl Nervonate	0.011	<41.2 [f]	870 [f]	<8.23 [f]	>125[f]

[a](Okoro et al., 2017a); [b,c](Ramírez-Verduzco et al., 2012) ; [d](Ramírez Verduzco, 2013); [e](Knothe, 2014); [f](Knothe, 2005)

Employing the methods described in section 2 above, the fuel properties of the FAME mixture in the present study were estimated and presented in Table 6.

Table 6: Biodiesel properties of the BWME compared to biodiesel standards

Properties	Units	EN14214	ASTMD6751-12	SBME	BWME
Density at 15°C	kg/m^3	860-900[c]	880[c]	885[b]	871.21
Viscosity at 40°C	mm^2/s	3.5-5.0[c]	1.9-6.0[c]	4.2[a]	4.14
Flash point	°C	≥101[c]	≥130[c]	186.5[j]	164.12
Cetane number	/	≥51[c]	≥ 47[c]	46[b]	73.57
Cloud point	°C	NS	-3 to -12[c]	1[b]	-4.27
CFPP	°C	NS	max 5[c]	-5[a]	-7.25
HHV	MJ/kg	>35	NS	40[b]	38.61

SBME denotes soybean methyl ester; [a](Cavalheiro et al., 2020); [b](Atabani et al., 2013); [c](Sakthivel et al., 2018); NS denotes not specified

The properties of the FAME mixture compared to the European (EN14214) and American (ASTM D6751-20) biodiesel standard properties and the properties of biodiesel produced from soybeans are also presented in Table 6. Soybean biodiesel has been considered since it is a commonly utilized feedstock for high-grade biodiesel production (Okoro et al., 2017a). Table 6 shows that the BWME satisfies the conditions imposed by European and American standards. Notably, the result suggests that the BWME mixture performed better than the soybean biodiesel with respect to the cold flow properties of CP and CFPP. This is because the BWME was dominated by medium-chain FAMEs which produce a biodiesel product characterized by improved viscosity

and favorable cold flow properties (Foon et al., 2006; Hoekman et al., 2012; Knothe, 2005) as stated above. The low level of unsaturation (i.e. ~29 % molar basis), a reduction in the oxidation rates and a reduction in the risk of NO_x emission (Foon et al., 2006; Imahara et al., 2006) (Knothe, 2005). The mole fraction of all saturated FAMEs (i.e. ~71 % molar basis) is also responsible for the high and favorable levels of CN (i.e. 72.89) and HHV(i.e. 39.02) calculated.

3.7 Economic performance

Using the methods described in section 2.5 and the cost components calculated as presented in Figure 5.

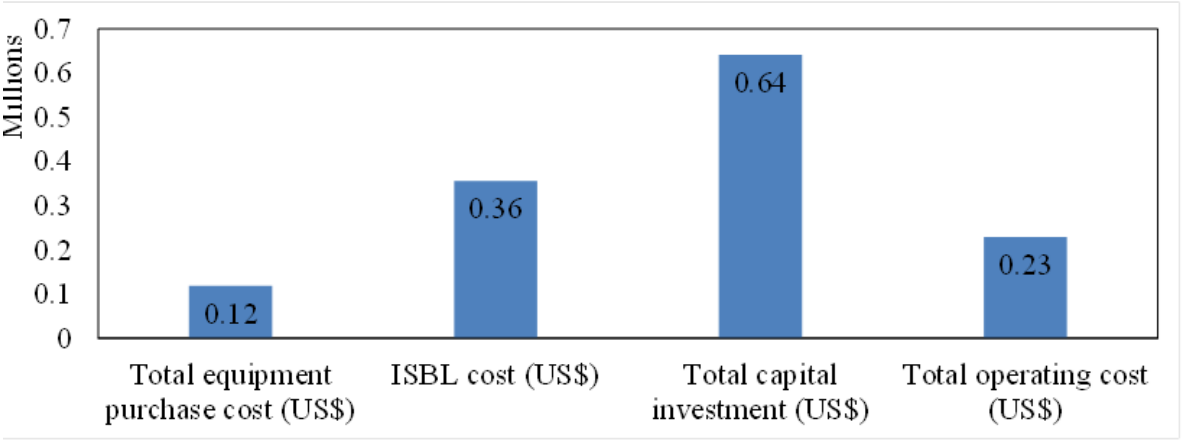

Figure 5 : Cost components of the proposed insect farming waste stream valorization process

Based on the data presented in Figure 5, the unit processing cost can be estimated and presented in Figure 6.

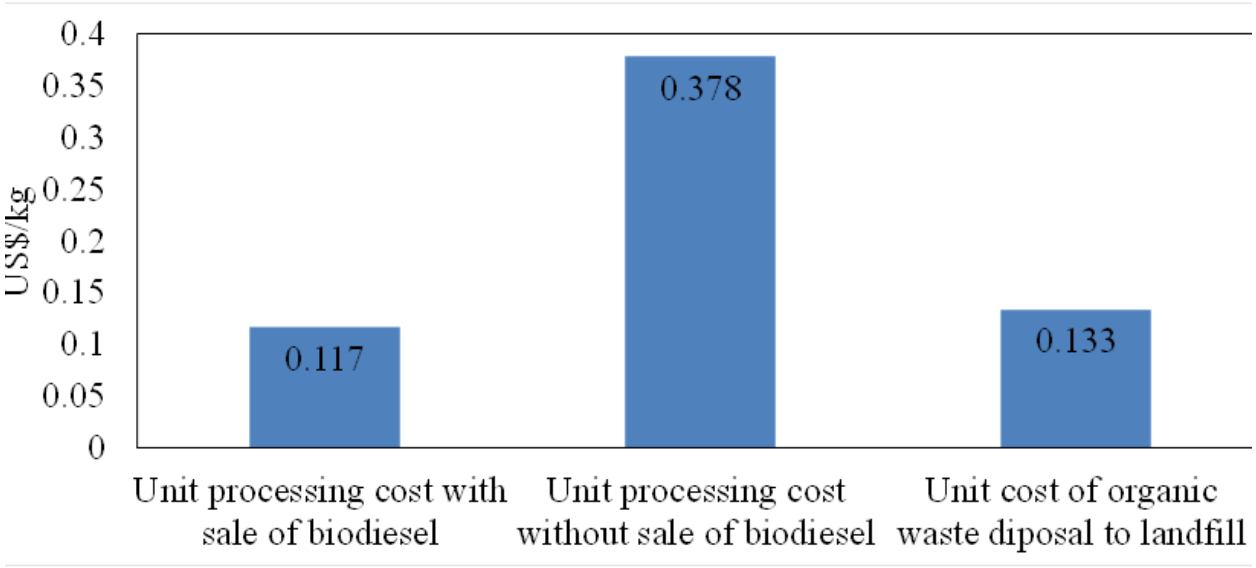

Figure 6 : Comparative unit processing cost of insect farming waste

Figure 6 shows that the unit processing cost of the insect farming waste, when biodiesel is not sold and when biodiesel is sold, which in for case 2 are less than the landfill cost of US$0.133 per kg reported in section 2.5. This highlights the potential economic benefits of exploring the waste valorisation for biodiesel production rather than disposal to landfills. It is acknowledged that this result is essentially a 'first-level' assessment and may be optimistic since some costs were not considered e.g., cost due to recovery of excess methanol. Notably, although the economic calculation results are dependent on the underlying cost assumptions, the results herein present a compelling argument to further explore insect farming waste valorisation for biodiesel production. Furthermore, the potential for producing secondary protein dense product streams should be explored in future works as a viable revenue source.

4 Conclusions

The present work employed subcritical water extraction (SWE) technology to maximize the fractionation of insects farming waste stream for lipid extraction using the response surface methodology. The optimally extracted lipids were successfully transesterified and the resulting BWME mixture was estimated to possess properties that satisfied the requirements imposed by the EN14214 and ASTM D6751-12 biodiesel standards. The dominance of moderate-length carbon chains present in the FAMEs was identified as responsible for the favorable cold flow properties, which according to the literature constitutes a common hindrance to widespread biodiesel application. The waste was further assessed as a potential source of high-value useful bioactive, i.e., oligopeptides, with further work in this area proposed. Finally, preliminary costing of the valorisation process showed that the process facilitates the waste management at a lower cost compared to the mean cost of disposal of organic waste to landfills in Belgium. While this study demonstrates the experimental viability of biodiesel production from the insect farming waste stream, it is acknowledged that more research is required in the area of the energy demand of SWE versus yield optimization and the undertaking of a more accurate economic viability study of the biodiesel production process, using process simulation tools such as ASPEN plus to assess its scalability.

Declaration of Competing Interest

The authors declare that they have no known competing financial interests or personal relationships that could have appeared to influence the work reported in this paper.

Acknowledgments

The authors also acknowledge FNRS-Fonds de la Recherche Scientifique for projets bilatéraux de mobilité (PINT-BILAT-M):/VA-R M005.21. The assistance of Celine Mornard (ULB) in conceptualizing and developing the graphical abstract is also acknowledged.

References

Agarwal, M., Singh, K., Chaurasia, S.P. 2010. Prediction of Biodiesel Properties from Fatty Acid Composition using Linear Regression and ANN Techniques. *Indian Chemical Engineer*, **52**(4), 347-361.

Akhtar, J., Amin, N.A.S. 2011. A review on process conditions for optimum bio-oil yield in hydrothermal liquefaction of biomass. *Renewable and Sustainable Energy Reviews*, **15**(3), 1615-1624.

Alviso, D., Artana, G., Duriez, T. 2020. Prediction of biodiesel physico-chemical properties from its fatty acid composition using genetic programming. *Fuel*, **264**, 116844.

AOAC. 1998. Combustion Method for Determination of Crude Protein in Animal Feeds, Oilseed Meals and Oilseeds. American Oil Chemists Society.

AOAC. 2012. Official Methods of Analysis of AOAC International (19th ed.). AOAC International Gaithersburg, MD, USA.

ASTM. 1998. D2017 - 98 Standard Test Method of Accelerated Laboratory Test of Natural Decay Resistance of Woods , decay, evaluation, laboratory, natural, resistance and subjected to termite bioassay according to no-choice test procedure based upon AWPA E1-97 (AWPA, 1. American Society for Testing and Materials.

ASTM. 2007. D3172-07 Standard Practice for Proximate Analysis of Coal and Coke. American Society for Testing and Materials.

ASTM. 2015. *Standard Test Method for Determination of Total Solids in Biomass*. ASTM International, West Conshohocken.

ASTM. 2011. Standard Test Method for Volatile Matter in the Analysis Sample of Coal and Coke,. American Society for Testing and materials International.

Atabani, A.E., Mahlia, T.M.I., Masjuki, H.H., Badruddin, I.A., Yussof, H.W., Chong, W.T., Lee, K.T. 2013. A comparative evaluation of physical and chemical properties of biodiesel synthesized from edible and non-edible oils and study on the effect of biodiesel blending. *Energy*, **58**, 296-304.

Baicu, A.A. 2022. Chapter 7 - Regulating emerging food trends: a case study in insects as food for humans. in: *Ensuring Global Food Safety (Second Edition)*, (Eds.) A. Martinović, S. Oh, H. Lelieveld, Academic Press, pp. 167-173.

Batish, I., Brits, D., Valencia, P., Miyai, C., Rafeeq, S., Xu, Y., Galanopoulos, M., Sismour, E., Ovissipour, R. 2020. Effects of Enzymatic Hydrolysis on the Functional Properties, Antioxidant Activity and Protein Structure of Black Soldier Fly (Hermetia illucens) Protein. *Insects*, **11**(12), 876.

Benjumea, P., Agudelo, J., Agudelo, A. 2008. Basic properties of palm oil biodiesel–diesel blends. *Fuel*, **87**(10), 2069-2075.
Bogusz, R., Smetana, S., Wiktor, A., Parniakov, O., Pobiega, K., Rybak, K., Nowacka, M. 2022. The selected quality aspects of infrared-dried black soldier fly (Hermetia illucens) and yellow mealworm (Tenebrio molitor) larvae pre-treated by pulsed electric field. *Innovative Food Science & Emerging Technologies*, **80**, 103085.
Bordin, K., Tomihe Kunitake, M., Kazue Aracava, K., Silvia Favaro Trindade, C. 2013. Changes in food caused by deep fat frying - A review %J Archivos Latinoamericanos de Nutrición. **63**, 5-13.
Brigode, C., Hobbi, P., Jafari, H., Verwilghen, F., Baeten, E., Shavandi, A. 2020. Isolation and physicochemical properties of chitin polymer from insect farm side stream as a new source of renewable biopolymer. *Journal of Cleaner Production*, **275**, 122924.
Brunelle, J.L., Green, R. 2014. One-dimensional SDS-Polyacrylamide Gel Electrophoresis (1D SDS-PAGE). in: *Methods in Enzymology*, Vol. 541, pp. 151-159.
Caligiani, A., Marseglia, A., Leni, G., Baldassarre, S., Maistrello, L., Dossena, A., Sforza, S. 2018. Composition of black soldier fly prepupae and systematic approaches for extraction and fractionation of proteins, lipids and chitin. *Food Research International*, **105**, 812-820.
Cavalheiro, L.F., Misutsu, M.Y., Rial, R.C., Viana, L.H., Oliveira, L.C.S. 2020. Characterization of residues and evaluation of the physico chemical properties of soybean biodiesel and biodiesel: Diesel blends in different storage conditions. *Renewable Energy*, **151**, 454-462.
Chemanalyst. 2023. Sulphuric acid pricing Chemanalyst.
Cholewski, M., Tomczykowa, M., Tomczyk, M. 2018. A Comprehensive Review of Chemistry, Sources and Bioavailability of Omega-3 Fatty Acids. *Nutrients*, **10**(11).
Clements, D. 1996. Biending Kules for Formulating Biodiesel Fuel. *Liquid Fuel and Industrial Products from Renewable Resources.*, 44-53.
Costa, N.R., Lourenço, J., Pereira, Z.L. 2011. Desirability function approach: A review and performance evaluation in adverse conditions. *Chemometrics and Intelligent Laboratory Systems*, **107**(2), 234-244.
Demirbas, A. 2007. Mathematical Relationships Derived from Biodiesel Fuels. *Energy Sources, Part A: Recovery, Utilization, and Environmental Effects*, **30**(1), 56-69.
Derringer, G., Suich, R. 1980. Simultaneous Optimization of Several Response Variables. *Journal of Quality Technology*, **12**(4).
Dortmans, B., Diener, S., Verstappen, B., Zurbrügg, C. 2017. Black Soldier Fly Biowaste Processing. 100.
Dunn, R.O., Bagby, M.O. 1995. Low-temperature properties of triglyceride-based diesel fuels: Transesterified methyl esters and petroleum middle distillate/ester blends. *Journal of the American Oil Chemists' Society*, **72**(8), 895-904.
EEA. 2013. Typical charge (gate fee and landfill tax) for legal landfilling of non-hazardous municipal waste in EU Member States and regions. European Environmental Agency.
Ehimen, E.A., Sun, Z.F., Carrington, C.G. 2010. Variables affecting the in situ transesterification of microalgae lipids. *Fuel*, **89**(3), 677-684.
EngineeringToolBox. 2018. Methanol - Specific Heat vs. Temperature and Pressure. EngineeringToolBox.

Ewald, N., Vidakovic, A., Langeland, M., Kiessling, A., Sampels, S., Lalander, C. 2020. Fatty acid composition of black soldier fly larvae (Hermetia illucens) – Possibilities and limitations for modification through diet. *Waste Management*, **102**, 40-47.

Faizollahzadeh Ardabili, S., Najafi, B., Shamshirband, S. 2019. Fuzzy logic method for the prediction of cetane number using carbon number, double bounds, iodic, and saponification values of biodiesel fuels. **38**(2), 584-599.

Foon, C.S., Liang, Y.C., Mat Dian, N.L.H., May, C.Y., Hock, C.C., Ngan, M.A. 2006. Crystallisation and Melting Behavior of Methyl Esters of Palm Oil. *American Journal of Applied Sciences*, **3**(5), 1859-1863.

Giakoumis, E.G., Sarakatsanis, C.K. 2018. Estimation of biodiesel cetane number, density, kinematic viscosity and heating values from its fatty acid weight composition. *Fuel*, **222**, 574-585.

Giannetto, A., Oliva, S., Ceccon Lanes, C.F., de Araújo Pedron, F., Savastano, D., Baviera, C., Parrino, V., Lo Paro, G., Spanò, N.C., Cappello, T., Maisano, M., Mauceri, A., Fasulo, S. 2020. Hermetia illucens (Diptera: Stratiomydae) larvae and prepupae: Biomass production, fatty acid profile and expression of key genes involved in lipid metabolism. *Journal of Biotechnology*, **307**, 44-54.

GPP. 2023. Natural gas prices globalpetrolprices.com.

Haghighi, A., Khajenoori, M. 2013. Subcritical Water Extraction. in: *Mass Transfer - Advances in Sustainable Energy and Environment Oriented Numerical Modeling*, (Eds.) H. Nakajima, H. Nakajima.

He, S., Lian, W., Liu, X., Xu, W., Wang, W., Qi, S. 2022. Transesterification synthesis of high-yield biodiesel from black soldier fly larvae by using the combination of Lipase Eversa Transform 2.0 and Lipase SMG1. *Food science and Technology*, **42**.

Ho, B.C.H., Kamal, S.M.M., Danquah, M.K., Harun, R. 2018. Optimization of Subcritical Water Extraction (SWE) of Lipid and Eicosapentaenoic Acid (EPA) from Nannochloropsis gaditana. *BioMed Research International*, **2018**, 1-11.

Hobbi, P., Okoro, O.V., Hajiabbas, M., Hamidi, M., Nie, L., Megalizzi, V., Musonge, P., Dodi, G., Shavandi, A. 2023. Chemical Composition, Antioxidant Activity and Cytocompatibility of Polyphenolic Compounds Extracted from Food Industry Apple Waste: Potential in Biomedical Application. **28**(2), 675.

Hoekman, S.K., Broch, A., Robbins, C., Ceniceros, E., Natarajan, M. 2012. Review of biodiesel composition, properties, and specifications. *Renewable and Sustainable Energy Reviews*, **16**(1), 143-169.

Humbird, D., Davis, R., Tao, L., Kinchin, C., Hsu, D., Aden, A., Schoen, P., Lukas, J., Olthof, B., Worley, M. 2011. Process design and economics for biochemical conversion of lignocellulosic biomass to ethanol: dilute-acid pretreatment and enzymatic hydrolysis of corn stover. National Renewable Energy Lab.(NREL), Golden, CO (United States).

Ilham, Z. 2022. Biomass classification and characterization for conversion to biofuels. in: *Value-Chain of Biofuels*, pp. 69-87.

Imahara, H., Minami, E., Saka, S. 2006. Thermodynamic study on cloud point of biodiesel with its fatty acid composition☆. *Fuel*, **85**(12-13), 1666-1670.

Islam, M.A., Ayoko, G.A., Brown, R., Stuart, D., Heimann, K. 2013. Influence of Fatty Acid Structure on Fuel Properties of Algae Derived Biodiesel. *Procedia Engineering*, **56**, 591-596.

Jung, S., Jung, J.-M., Tsang, Y.F., Bhatnagar, A., Chen, W.-H., Lin, K.-Y.A., Kwon, E.E. 2022. Biodiesel production from black soldier fly larvae derived from food waste by non-catalytic transesterification. *Energy*, **238**, 121700.

Kim, J., Choi, K., Chung, D.S. 2012. 3.35 - Sample Preparation for Capillary Electrophoretic Applications. in: *Comprehensive Sampling and Sample Preparation*, (Ed.) J. Pawliszyn, Academic Press. Oxford, pp. 701-721.

Knothe, G. 2014. A comprehensive evaluation of the cetane numbers of fatty acid methyl esters. *Fuel*, **119**, 6-13.

Knothe, G. 2005. Dependence of biodiesel fuel properties on the structure of fatty acid alkyl esters. *Fuel Processing Technology*, **86**(10), 1059-1070.

Lalander, C., Diener, S., Zurbrügg, C., Vinnerås, B. 2019. Effects of feedstock on larval development and process efficiency in waste treatment with black soldier fly (Hermetia illucens). *Journal of Cleaner Production*, **208**, 211-219.

Liu, T., Klammsteiner, T., Dregulo, A.M., Kumar, V., Zhou, Y., Zhang, Z., Awasthi, M.K. 2022. Black soldier fly larvae for organic manure recycling and its potential for a circular bioeconomy: A review. *Science of The Total Environment*, **833**, 155122.

Madau, F.A., Arru, B., Furesi, R., Pulina, P. 2020. Insect Farming for Feed and Food Production from a Circular Business Model Perspective. **12**(13), 5418.

Methanex. 2023. Methanol Priceing Methanex.

Myers, H., Tomberlin, Lambert, iB. 2008. Development of black soldier fly (Diptera: Stratiomyidae) larvae fed dairy manure.

Nguyen, H.C., Liang, S.-H., Li, S.-Y., Su, C.-H., Chien, C.-C., Chen, Y.-J., Huong, D.T.M. 2018. Direct transesterification of black soldier fly larvae (Hermetia illucens) for biodiesel production. *Journal of the Taiwan Institute of Chemical Engineers*, **85**, 165-169.

Oh, Y.-K., Hwang, K.-R., Kim, C., Kim, J.R., Lee, J.-S. 2018. Recent developments and key barriers to advanced biofuels: A short review. *Bioresource Technology*, **257**, 320-333.

Okoro, O.V., Nie, L., Waeytens, J., Hamidi, M., Shavandi, A. 2022. Thermochemical Liquefaction of Pomace Using Sub/Supercritical Ethanol: an Integrated Experimental and Preliminary Economic Feasibility Study. *J Bioenergy Research*, 1-13.

Okoro, O.V., Sun, Z., Birch, J. 2017a. Meat processing dissolved air flotation sludge as a potential biodiesel feedstock in New Zealand: A predictive analysis of the biodiesel product properties. *Journal of Cleaner Production*, **168**, 1436-1447.

Okoro, O.V., Sun, Z., Birch, J. 2017b. Meat processing waste as a potential feedstock for biochemicals and biofuels – A review of possible conversion technologies. *Journal of Cleaner Production*, **142**, 1583-1608.

Okoro, O.V., Sun, Z., Birch, J. 2019. Techno-Economic Assessment of a Scaled-Up Meat Waste Biorefinery System: A Simulation Study. **12**(7), 1030.

Pandey, K., Yadav, A.K., Goel, C. 2022. Utilization of Food Waste for Biofuel Production. in: *Food Waste to Green Fuel: Trend & Development*, (Eds.) N. Srivastava, M.A. Malik, Springer Nature Singapore. Singapore, pp. 1-23.

Park, J.-S., Han, J.-M., Surendhiran, D., Chun, B.-S. 2022. Physicochemical and biofunctional properties of Sargassum thunbergii extracts obtained from subcritical water extraction and conventional solvent extraction. *The Journal of Supercritical Fluids*, **182**, 105535.

Pavlić, B., Vidović, S., Vladić, J., Radosavljević, R., Cindrić, M., Zeković, Z. 2016. Subcritical water extraction of sage (Salvia officinalis L.) by-products—Process optimization by response surface methodology. *The Journal of Supercritical Fluids*, **116**, 36-45.

Polikovsky, M., Gillis, A., Steinbruch, E., Robin, A., Epstein, M., Kribus, A., Golberg, A. 2020. Biorefinery for the co-production of protein, hydrochar and additional co-products from a green seaweed Ulva sp. with subcritical water hydrolysis. *Energy Conversion and Management*, **225**, 113380.

Purkayastha, D., Sarkar, S. 2021. Sustainable waste management using black soldier fly larva: a review. *International Journal of Environmental Science and Technology*.

Ramírez-Verduzco, L.F., Rodríguez-Rodríguez, J.E., Jaramillo-Jacob, A.d.R. 2012. Predicting cetane number, kinematic viscosity, density and higher heating value of biodiesel from its fatty acid methyl ester composition. *Fuel*, **91**(1), 102-111.

Ramírez Verduzco, L.F. 2013. Density and viscosity of biodiesel as a function of temperature: Empirical models. *Renewable and Sustainable Energy Reviews*, **19**, 652-665.

Ramos, M.J., Fernández, C.M., Casas, A., Rodríguez, L., Pérez, Á. 2009. Influence of fatty acid composition of raw materials on biodiesel properties. *Bioresource Technology*, **100**(1), 261-268.

Ravi, H.K., Degrou, A., Costil, J., Trespeuch, C., Chemat, F., Vian, M.A. 2020. Larvae Mediated Valorization of Industrial, Agriculture and Food Wastes: Biorefinery Concept through Bioconversion, Processes, Procedures, and Products. *Processes*, **8**(7), 857.

Reddy, H.K., Muppaneni, T., Sun, Y., Li, Y., Ponnusamy, S., Patil, P.D., Dailey, P., Schaub, T., Holguin, F.O., Dungan, B. 2014. Subcritical water extraction of lipids from wet algae for biodiesel production. *Fuel*, **133**, 73-81.

Rodríguez-Meizoso, I., Jaime, L., Santoyo, S., Señoráns, F.J., Cifuentes, A., Ibáñez, E. 2010. Subcritical water extraction and characterization of bioactive compounds from Haematococcus pluvialis microalga. *Journal of Pharmaceutical and Biomedical Analysis*, **51**(2), 456-463.

Sakthivel, R., Ramesh, K., Purnachandran, R., Mohamed Shameer, P. 2018. A review on the properties, performance and emission aspects of the third generation biodiesels. *Renewable and Sustainable Energy Reviews*, **82**, 2970-2992.

Salsinha, A.S., Machado, M., Rodríguez-Alcalá, L.M., Gomes, A.M., Pintado, M. 2023. Chapter 1 - Bioactive lipids: Chemistry, biochemistry, and biological properties. in: *Bioactive Lipids*, (Eds.) M. Pintado, M. Machado, A.M. Gomes, A.S. Salsinha, L.M. Rodríguez-Alcalá, Academic Press, pp. 1-35.

Sánchez, A., Vázquez, A. 2017. Bioactive peptides: A review. *Food Quality and Safety*, **1**(1), 29-46.

Sarin, A., Arora, R., Singh, N.P., Sarin, R., Malhotra, R.K., Kundu, K. 2009. Effect of blends of Palm-Jatropha-Pongamia biodiesels on cloud point and pour point. *Energy*, **34**(11), 2016-2021.

Schaich, K.J.L.o.p. 2008. Chapter 8: Co-oxidations of oxidizing lipids: Reactions with proteins. 183-274.

Serrano, R., Navarro, J.C., Sales, C., Portolés, T., Monroig, Ó., Beltran, J., Hernández, F. 2022. Determination of very long-chain polyunsaturated fatty acids from 24 to 44 carbons in eye, brain and gonads of wild and cultured gilthead sea bream (Sparus aurata). *Scientific Reports*, **12**(1), 10112.

Su, C.-H., Nguyen, H.C., Bui, T.L., Huang, D.-L. 2019. Enzyme-assisted extraction of insect fat for biodiesel production. *Journal of Cleaner Production*, **223**, 436-444.

Surendra, K.C., Tomberlin, J.K., van Huis, A., Cammack, J.A., Heckmann, L.-H.L., Khanal, S.K. 2020. Rethinking organic wastes bioconversion: Evaluating the potential of the black soldier fly (Hermetia illucens (L.)) (Diptera: Stratiomyidae) (BSF). *Waste Management*, **117**, 58-80.

Suzihaque, M.U.H., Alwi, H., Kalthum Ibrahim, U., Abdullah, S., Haron, N. 2022. Biodiesel production from waste cooking oil: A brief review. *Materials Today: Proceedings*, **63**, S490-S495.

Talent. 2023. Factory Worker average salary in the USA, 2023. www.talent.com.

Vardon, D.R., Sharma, B.K., Blazina, G.V., Rajagopalan, K., Strathmann, T.J. 2012. Thermochemical conversion of raw and defatted algal biomass via hydrothermal liquefaction and slow pyrolysis. *Bioresource Technology*, **109**, 178-187.

Velayi, E., Norouzbeigi, R. 2023. Fabrication of epoxy/SiO2/ZnO superhydrophobic nanocomposite mesh membranes for oil-water separation: Correlating oil flux to fabrication parameters via Box-Behnken design. *Applied Surface Science*, **611**, 155594.

Viswanathan, M.B., Cheng, M.-H., Clemente, T.E., Dweikat, I., Singh, V. 2021. Economic perspective of ethanol and biodiesel coproduction from industrial hemp. *Journal of Cleaner Production*, **299**, 126875.

Wang, Y., Wang, C., Zhao, J., Ding, Y., Li, L. 2017. A cost-effective method to prepare curcumin nanosuspensions with enhanced oral bioavailability. *Journal of Colloid and Interface Science*, **485**, 91-98.

worldbank. 2023. Trends in Solid Waste Management. The world bank.

Yang, M., Chen, L., Wang, J., Msigwa, G., Osman, A.I., Fawzy, S., Rooney, D.W., Yap, P.-S. 2023. Circular economy strategies for combating climate change and other environmental issues. *Environmental Chemistry Letters*, **21**(1), 55-80.

Zeković, Z., Vidović, S., Vladić, J., Radosavljević, R., Cvejin, A., Elgndi, M.A., Pavlić, B. 2014. Optimization of subcritical water extraction of antioxidants from Coriandrum sativum seeds by response surface methodology. *The Journal of Supercritical Fluids*, **95**, 560-566.

Zheng, L., Li, Q., Zhang, J., Yu, Z. 2012. Double the biodiesel yield: Rearing black soldier fly larvae, Hermetia illucens, on solid residual fraction of restaurant waste after grease extraction for biodiesel production. *Renewable Energy*, **41**, 75-79.

Zhou, F., Tomberlin, J.K., Zheng, L., Yu, Z., Zhang, J. 2013. Developmental and Waste Reduction Plasticity of Three Black Soldier Fly Strains (Diptera: Stratiomyidae) Raised on Different Livestock Manures. *Journal of Medical Entomology*, **50**(6), 1224-1230.